Charge disproportionation and Jahn-Teller distortion in $LiNiO_2$ and $NaNiO_2$: A density functional theory study

Hungru Chen,* Colin L. Freeman, and John H. Harding
Department of Materials Science and Engineering, University of Sheffield, S1 3JD, United Kingdom
(Received 24 March 2011; revised manuscript received 12 July 2011; published 19 August 2011)

Density functional theory calculations have been performed on three potential ground-state configurations of $LiNiO_2$ and $NaNiO_2$. These calculations show that, whereas $NaNiO_2$ shows the expected cooperative Jahn–Teller distortion (and therefore a crystal structure with $C2/m$ symmetry), $LiNiO_2$ shows at least two possible crystal structures very close in energy (within 3 meV/formula unit): $P2_1/c$ and $P2/c$. Moreover, one of them ($P2/c$) shows charge disproportionation of the (expected) Ni^{3+} cations into Ni^{2+} and Ni^{4+}. We discuss the implications of this complex ground state for the interpretation of the available electron and neutron structure data, its electronic and complex magnetic behavior.

DOI: 10.1103/PhysRevB.84.085108 PACS number(s): 71.15.Mb

I. INTRODUCTION

$LiNiO_2$ has attracted considerable interest due to its potential application as a cathode material in lithium ion batteries. Although this compound has been intensively studied for many years, the local geometry and electronic and magnetic structure are still highly debatable. The analysis of the data is complicated by the well-known difficulty of synthesizing truly stoichiometric $LiNiO_2$. Experimentally, both Ni^{2+} and Ni^{3+} in $LiNiO_2$ have been reported using various detection techniques.[1–4] Even the most recent experimental studies struggle to obtain truly stoichiometric material. Where quoted, typical defect concentrations are of the order of a few percent; nickel is found on the lithium site of the perfect structure.[5]

Unlike the analogous sodium compound, $NaNiO_2$, $LiNiO_2$ shows neither long-range magnetic order nor a long-range cooperative Jahn–Teller effect despite the fact that all calculations until now (for example Refs. 6 and 7) in $LiNiO_2$ show that Ni is present as low-spin Ni^{3+} with an electronic configuration $t_2g^6e_g^1$ which is Jahn–Teller active. Two different Ni-O bond lengths have been observed, both in EXAFS[8,9] and neutron diffraction,[5] which are attributed to a local Jahn–Teller distortion, unlike the cooperative distortion seen in other Jahn–Teller active systems, such as $NaNiO_2$ and $LiMnO_2$. The analysis of the neutron partial density function (PDF) in Ref. 5 supports the hypothesis of a Jahn–Teller distortion since their results show four bond lengths grouped as long bonds (2.04 Å and 2.06 Å with an average length of 2.05 Å) and short bonds (1.90 Å and 1.96 Å with an average length of 1.93 Å) suggestive of the 2:1 ratio of short-to-long bonds expected for Jahn–Teller distortion. However, the long-range PDF peaks increase in height with temperature, an unusual effect that the authors attribute to domain formation.

The magnetic properties of $LiNiO_2$ have been a matter of debate since the first measurements in 1958.[10] Reynard *et al.*[11] suggested, on the basis of anomalies in the spin susceptibility observed at 10 and 400 K, that there were at least two energy scales involved, corresponding to spin and orbital interactions, and that the possibility of orbital frustration should be considered. The neutron studies of Ref. 5 argue against this since this would imply that the number of short and long Ni-O bonds would be equal. The authors suggest instead that the magnetic properties should be explained by the assumption that there is local orbital ordering: the $3d_{z^2-r^2/3}$ orbitals of three Ni^{3+} ions point towards their shared oxygen. This model also receives support from a recent electron diffraction study.[12] However, there remain problems with the interpretation of the magnetic data using this scheme; in particular the coexistence of ferromagnetic and antiferromagnetic spin fluctuations. It is argued[5] that the existence of domains, required to prevent stress buildup caused by the trimer ordering, may restrict the antiferromagnetic fluctuations. A recent set of first-principles density functional theory (DFT + U) calculations has been performed on the possible local orderings for Jahn–Teller distortions in $LiNiO_2$.[13]

However, a whole range of possible electronic ground states are possible in compounds that have a nominal Ni^{3+} charge state, from a totally delocalized metal ($LaNiO_3$) to a strongly localized orbital ordering insulator ($NaNiO_2$). This is shown in Table I where the behavior is correlated with the nickel-oxygen bond length (d_{Ni-O}).

Charge disproportionation is also reported for other rare earth nickelates.[20] It can be seen from the above table that in the case of $LiNiO_2$ there could be a competition between charge ordering and orbital ordering for the ground state. The purpose of this paper is to demonstrate that this is indeed the case using first-principles density functional theory and to discuss the consequences.

II. THEORETICAL METHODS

$LiNiO_2$ is frequently reported to crystallize in the hexagonal structure with $R\bar{3}m$ space group symmetry. A slight monoclinic distortion was observed at low temperatures (10 K) by the neutron diffraction study of Ref. 5 and a better fit found to the $C2/m$ space group, but detailed analysis showed that the collinear ordering of the Jahn–Teller distortions implied by this space group was not supported by a combination of the Rietveld refinement and the neutron PDF data. The electron diffraction study of Ref. 12 was analyzed using the Pm space group (which is the simplest space group that can incorporate a trimer ordering model).

A considerable amount of work has been done on both lithium-doped NiO and $LiNiO_2$ [which can be viewed as a special case of lithium-doped NiO where the doping level is 50%,

 ©2011 American Physical Society

TABLE I. The Ni-O bond lengths (d_{Ni-O}) in compounds with the nominal valence state Ni^{3+} compounds and their ground-state behavior. Numbers of Ni-O bonds of a given length are shown in brackets.

Compound	d_{Ni-O} (Å)	$\langle d_{Ni-O}\rangle$(Å)	Electronic ground state
$LaNiO_3$[14]	1.93 [6]	1.93	Metallic (delocalized)
$NdNiO_3$[15]	1.93[2], 1.94[2], 1.96[2]	1.94	Charge ordering insulator
$LuNiO_3$[16]	1.89[2], 1.92[2], 1.94[2] 1.97[2], 2.00[2], 2.02[2]	1.96	Charge ordering insulator
$YNiO_3$[17]	1.90[2], 1.92[2], 1.94[2] 1.96[2], 2.01[2], 2.01[2]	1.96	Charge ordering insulator
$AgNiO_2$[18]	1.95 [6]	1.95	Moderately charge ordering, $3Ni^{3+} \rightarrow Ni^{2+} + 2Ni^{3.5+}$
$LiNiO_2$[5]	1.90[4], 1.96[4], 2.04[2], 2.06[2]	1.97*	
$NaNiO_2$[19]	1.92[4], 2.15[2]	2.00	Orbital ordering insulator

*Note that the Ni-O bond lengths differ between studies of $LiNiO_2$.

and the Li and Ni positions are ordered on the (111) planes]. Calculations on lithium-doped NiO have argued that the hole is localized on the oxygen ion,[21,22] a position supported by the interpretation of oxygen K-edge x-ray absorption spectra.[23] However, the considerable volume of calculations on $LiNiO_2$ is united in interpreting this compound as contained Ni^{3+} (see, for example, Refs. 6,7,13,24, and 25). This is reinforced by the extensive magnetic data now available.[11,26] None of this denies that there is considerable charge transfer between the nickel and oxygen, but it does assert that interpretations in terms of holes on the nickel ions make better sense of the data for $LiNiO_2$. The two interpretations are not unconnected, as Anisimov *et al.*[27] point out.

Previous density functional calculations[13,25] have predicted that distortions with $C2/m$ symmetry lower the cohesive energy but did not consider charge disproportionation. In order to investigate the various possible electronic relaxations in $LiNiO_2$, we have used four unit cells as starting configurations. Two of these, $R\bar{3}m$ and $C2/m$ cells (each with one formula unit) have been discussed before. In addition, two more cells are proposed and discussed below. One cell contains a zigzag Jahn–Teller orbital ordering of the Ni^{3+} ions (also discussed in Refs. 5 and 13) and has $P2_1/c$ symmetry with two formula units. The other cell, with $P2/c$ symmetry containing four formula units but retaining good agreement with the measured lattice parameters of the low temperature structure, was constructed for the charge disproportionation model. As far as we are aware, no attempt has been made to analyze the experimental data using the $P2/c$ space group. We have also investigated the Pm unit cell suggested by Cao *et al.*[12] (eight formula units), but as we shall show, when the cell geometry is optimized, it becomes indistinguishable from $C2/m$.

First-principles DFT calculations using the generalized gradient approximation (GGA) and the Perdew–Burke–Ernzerhof (PBE) functional[28] were performed using the projector-augmented wave (PAW)[29] method to investigate the ground-state crystal and electronic structure of $LiNiO_2$. It has been shown previously[30] that the simpler local density approximation cannot give the Jahn–Teller distortion. It is also well known that the GGA functional does not give the correct electronic description of strongly correlated systems, such as transition metal oxides. One possible solution is to perform calculations with full exchange. However, this requires large amounts of computer resources and is impractical for the size and number of calculations we need to perform. We have, however, performed a hybrid exchange calculation on the highest symmetry $\left(R\bar{3}m\right)$ cell as a check on the simpler method we intend to use.

This approximation, known to work well for these systems, is to include an onsite Coulomb interaction, the Hubbard U parameter, in the standard DFT calculations, known as the DFT + U method.[27,31] The rotational invariant form[31] of the DFT + U formalism was used and $U_{eff} = U - J$, the onsite correction, was set to be 6.5 eV for Ni $3d$ electrons adapted from a self-consistent calculation.[32] Other work[13] has used a smaller value of U_{eff}. It is, however, important to demonstrate that results of calculations are not strongly dependent on the value of the U parameter chosen, and we provide evidence for this below. The inclusion of the U parameter has been shown to successfully reproduce the charge disproportionation in $LiMn_2O_4$, $LuNiO_3$, $NdNiO_3$, and $YNiO_3$ and used to investigate possible charge-orbital orderings in Fe_3O_4.[18,33–36] The cutoff energy for plane waves was set at 500 eV. For all cells, the k-point spacing is less than 0.03 $Å^{-1}$ in the Brillouin zone. Convergence of the energy was confirmed for both these parameters. For geometry optimization, the force was converged to less than 0.01 eV-$Å^{-1}$ per ion. In all cases, the cells were fully optimized assuming the starting symmetry of the cell. All calculations were carried out using the Vienna *ab initio* simulation package (VASP).[37]

III. RESULTS AND DISCUSSION

We have calculated the structures and lattice energies of the four unit cells discussed above and present our results, both for the structure and relative energies of the cells (using the $R\bar{3}m$ cell as a baseline for convenience). The relative ordering of lattice energies for the four cases is independent of the choice of the U_{eff} value, provided that value falls in the range 5.5–7.0 eV, as shown in Fig. 1. Outside this range, the $P2/c$ is destabilized relative to the $C2/m$ and $P2_1/c$ cells. Previous work[13] using a smaller value of U_{eff} (4.5 eV) is still comparable since, as can be seen from Fig. 1, the relative energies of the $C2/m$ and $P2_1/c$ cells change little over a very wide range of U_{eff} values. Even for a value of U_{eff} as low as 4.5 eV, the $P2/c$ cell is comparable in energy with the $C2/m$ and

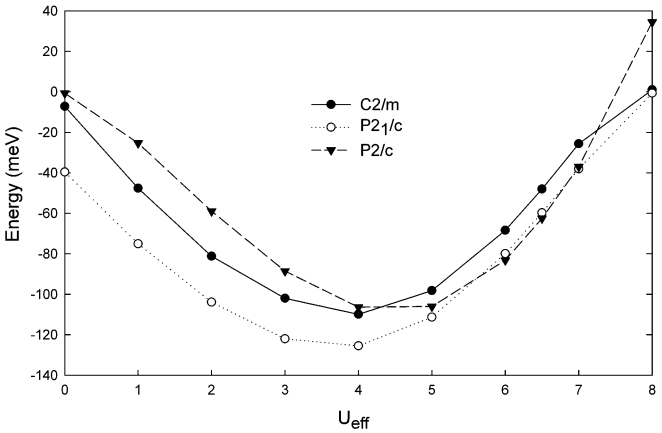

FIG. 1. Stabilization energies (relative to the $R\bar{3}m$ cell and given per formula unit) of the $C2/m$, $P2_1/c$, and $P2/c$ cells as a function of U_{eff}.

$P2_1/c$ cells. We note comparison with previous work where relevant (and consider only the fully relaxed cases), but our aim is rather different to theirs since we wish to consider whether the charge disproportionation cell can be lower than any Jahn–Teller ordering. Structural data for the cells is given in Table II for the chosen U_{eff} value of 6.5 eV. All further results use this value. It is convenient to consider the results for the unit cells in turn.

The cell parameters of the $R\bar{3}m$ cell are shown in Table II and demonstrate good agreement with the experimental values. Figure 1 shows the density of states of the $R\bar{3}m$ cell. The empty spin-up e_g band and half empty spin-down e_g band indicate an electronic configuration $t_2g^6e_g^1$, which corresponds to the d^7 state or Ni^{3+}. $LiNiO_2$ is reported to be a semiconductor with a band gap of about 0.5 eV,[39] but in the cell the spin-down e_g band lies on the Fermi level, which implies conducting behavior. The symmetry of the $R\bar{3}m$ cell ensures that all six Ni-O bonds are identical and disagrees with the observation of different Ni-O bond lengths seen in experiment.[5,8] We have also performed calculations using the screened hybrid functional HSE06[40] to compare with the DFT + U results.

This is shown in Fig. 2. Both methods predict that $LiNiO_2$ in this cell should be a metal because the half-filled e_g band includes the Fermi level. The main difference is the gap between the e_g band and the rest of the valence band states in the hybrid functional calculation. Both calculations show that the e_g states are a mixture of Ni and O character. They are not largely O character (as might be expected from the Hartree–Fock calculations on Li-doped NiO briefly discussed above). Also, the results show that the DFT + U calculations give a reasonable picture of the behavior of the system. For reasons of computational resources, it is not practical to perform full optimizations using the HSE06 functional for all the unit cells we consider.

In the optimized $C2/m$ cell, there are four short Ni-O bonds at 1.90 Å and two long Ni-O bonds at 2.14 Å, which corresponds to a Jahn–Teller distorted system. These results are in good agreement with the previous work of Refs. 13 and 25 (quoted as the $+Q_3$ mode). The total density of states of the $C2/m$ cell shown in Fig. 3 shows a split in the e_g band relating to a Jahn–Teller distortion. The band gap is approximately 0.5 eV, again in good agreement with the experimental data. Two unoccupied spin-up e_g states and one unoccupied spin-down e_g state are present, which indicates an electronic configuration $t_2g^6e_g^1$, or Ni^{3+}. This cell appears to be an accurate description for the Jahn–Teller relaxed structure generally accepted as the ground state of $LiNiO_2$. However, this cell presupposes a long-range cooperative Jahn–Teller distortion which is not observed.

In the $P2_1/c$ cell, all Ni ions are Jahn–Teller distorted with four short and two long Ni-O bonds, implying the presence of Ni^{3+} ions. The geometrical difference from the $C2/m$ cell is that the orientations of Jahn–Teller distortions in this cell are in a zigzag ordering. This induces, as expected,[5] significant distortion of the lattice from the $C2/m$ cell which is not observed in experiment. The results are similar to previous work;[13] the most notable change being that the monoclinic angle found here (125°) is significantly larger than previously (107.87°). From Fig. 3, the electronic structure of this $P2_1/c$ cell is almost identical to the $C2/m$ cell since the Ni ions are all Ni^{3+} in both cells. Nevertheless, it will be shown that this zigzag Jahn–Teller ordering is more stable than the collinear case. Calculations were also performed using the Pm cell (which represents a trimer ordering case) and coordinates of Ref. 12 as a starting point. Results without relaxation produced a cell of significantly higher energy (per formula unit) than the $R\bar{3}m$ cell. The higher energy of this structure may be due to the geometrical frustration identified by Ref. 5 resulting in significant strain in the structure. We are not able to relieve this strain by introducing the large-scale curvature suggested in Ref. 5; the number of atoms required for such a calculation are beyond what *ab initio* calculations can currently consider.

TABLE II. The optimized geometries of cells and calculated magnetic moments on nickel ions. Experimental values reported in brackets ($R\bar{3}m$[38]; $C2/m$[5], the Ni-O bond lengths quoted here are taken from the analysis of the Rietveldt refinement, not the neutron PDF analysis as discussed in the text below since this is not tied to the $C2/m$ symmetry).

Space group	a (Å)	b (Å)	c (Å)	β (°)	$d_{\text{Ni–O}}$ (Å)	Magnetic moment (μ_B)
$R\bar{3}m$	2.9023 (2.8788)		14.1889 (14.2035)		1.99[6] (1.974)	1.419
$C2/m$	5.151 (4.9693)	2.7929 (2.8774)	5.1461 (4.9967)	112.011 (109.204)	1.90[4], 2.14[2] (1.94[4], 1.96[2])	1.108
$P2_1/c$	5.8468	2.9302	4.90974	125.641	1.91[4], 2.12[2]	1.140
$P2/c$	5.0291	5.8059	4.942	70.6822	Ni(a) 2.05-2.07	Ni (a) 1.759
					Ni(b) 1.88-1.91	Ni (b) 0.128

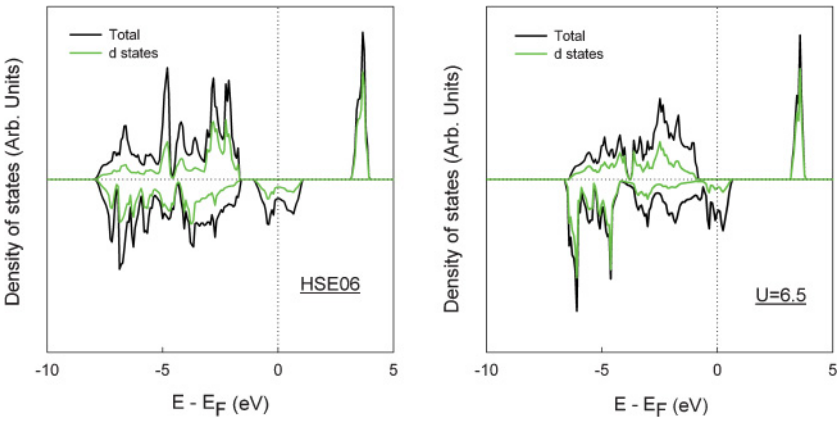

FIG. 2. (Color online) Comparison of (left) HSE06 functional and (right) DFT + U.

Upon geometrical relaxation, the Pm cell relaxed to a cell of $P2_1/c$ symmetry with the behavior discussed above. The issue of trimer ordering is considered in much more detail in Ref. 13.

The $P2/c$ cell contains four $LiNiO_2$ formula units and two inequivalent nickel sites in a zigzag ordering. The total density of states in Fig. 3 indicates that the $P2/c$ cell is a semiconductor with a band gap about 0.5 eV, in good agreement with the measured value. In the optimized geometry, Ni(a) has six long Ni-O bonds at 2.04 $\sim$ 2.07 Å with a magnetic moment of 1.759 μ_B. The local density of states in Fig. 4 shows that one e_g band is unoccupied (the spin-down band, but the choice is arbitrary), indicating the (high-spin) electronic configuration $t_2g^6e_g{}^2$ or Ni^{2+}. Ni(b) has six short Ni-O bond lengths at 1.88 $\sim$ 1.91 Å with a magnetic moments 0.128 μ_B. The local density of states in Fig. 4 for Ni(b) shows that both the spin-up and spin-down e_g bands are unoccupied, indicating the electronic configuration $t_2g^6e_g{}^0$ or low-spin Ni^{4+}.

Figure 5 shows the isosurface of the charge density difference, which demonstrates substantially different amounts of electron density on the two nickel ions. The $P2/c$ cell therefore shows charge disproportionation. Although not reported in experiments, the $P2/c$ cell reproduces the insulating character of $LiNiO_2$, and the amount of monoclinic distortion displayed is about 0.22°, in very good agreement with the value 0.16° detected by neutron diffraction at low temperature[5] in the sample assigned to $C2/m$ symmetry.

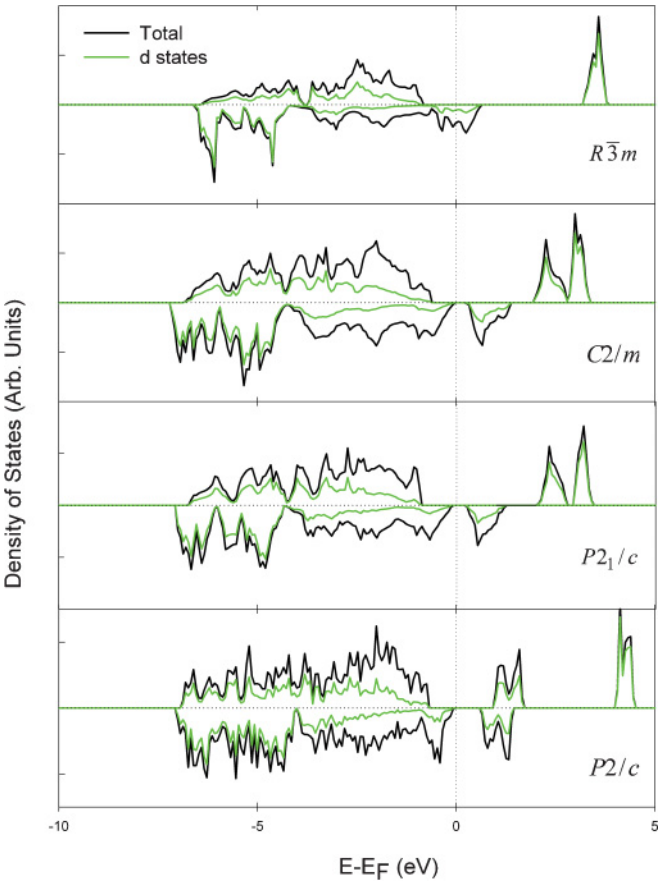

FIG. 3. (Color online) The density of states of the four candidate unit cells for $LiNiO_2$. Cells are indicated as above. Note that only the Jahn–Teller distorted ($C2/m$, $P2_1/c$) or charge disproportionating ($P2/c$) cells show semiconducting behavior.

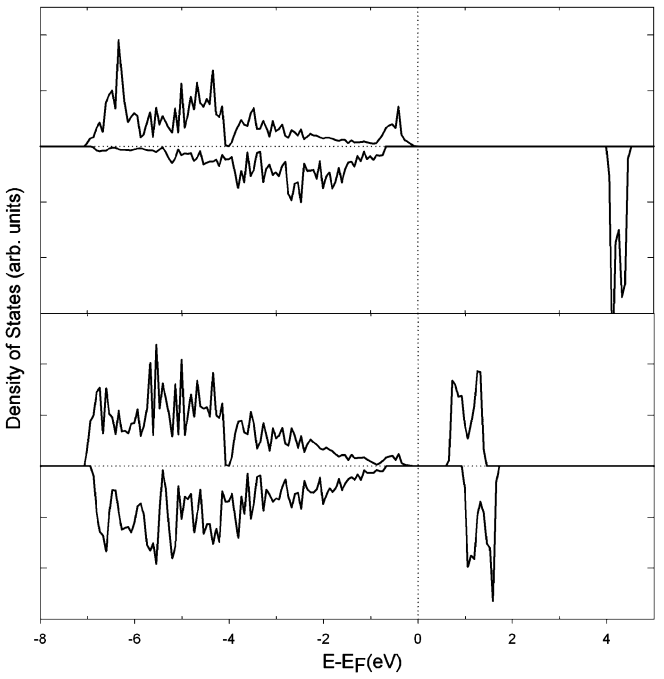

FIG. 4. Local density of states for the two inequivalent nickels in the $P2/c$ cell. The top diagram shows the nickel with six long Ni-O bonds. The bottom diagram shows the nickel with six short Ni-O bonds.

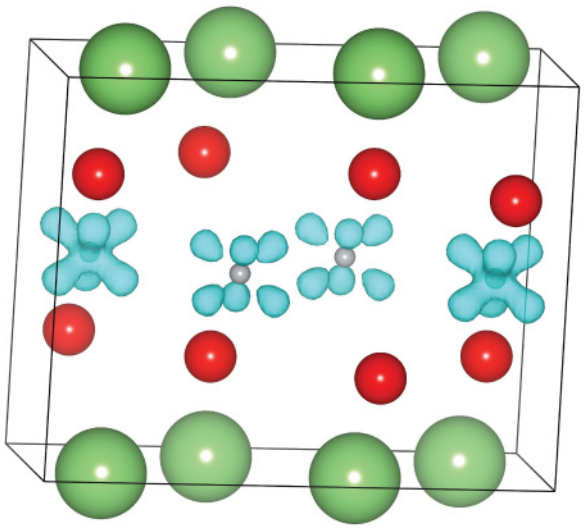

FIG. 5. (Color online) Charge-density difference map for the $P2/c$ cell. Green denotes Li, red denotes O, and grey denotes Ni. Note the differences between the two kinds of Ni atom.

We emphasize that, despite our simple denotation of the nickel charge states as Ni^{3+} and Ni^{4+}, there is considerable charge transfer between the nickel and oxygen ions. This is clear from the densities of states in Fig. 3 from looking at the amount of d character shown in the figures. A similar point is made by the Mulliken and Bader charges shown in Table III below.

The lattice energies of the four cells are listed in Table IV. The lowest energy cell for $LiNiO_2$ is that with $P2/c$ symmetry. This suggests that charge disproportionation must be considered as a reasonable mechanism to remove the orbital degeneracy of Ni^{3+} in $LiNiO_2$. The ordering of the other cells is the same as for previous work,[13] but the relative stabilization energies somewhat different, the ones quoted here are about twice those in Ref. 13. This can reasonably be ascribed to the different U_{eff} values used. The lattice energy of the $P2/c$ cell is, however, only about 2 meV lower than the $P2_1/c$ cell (the equivalent of 25 K and well within the margin of error of the calculation) and 14.5 meV lower than the $C2/m$ cell (the equivalent of 170 K and probably within the margin of error). Table IV also shows the lattice energies for $NaNiO_2$ in the three different symmetries explored for $LiNiO_2$. $NaNiO_2$, unlike $LiNiO_2$, is found exclusively in the Jahn–Teller relaxed state. Previous calculations[41] on the $R\bar{3}m$ and $C2/m$ cells of $NaNiO_2$ were performed using a U_{eff} value of 4.5 eV, but from Fig. 1 it is clear that similar results are expected for our value of 6.5 eV, except for the $P2/c$ disproportionation cell, which the previous work did not consider. Our calculations find the lowest-energy configuration to be the cooperative $C2/m$ Jahn–Teller cell by approximately 32 meV (and 58 meV below the charge-disproportionation cell $P2/c$). This is many times the energy difference between the lowest-energy Jahn–Teller cell and the charge disproportionation cell in $LiNiO_2$.

Our results suggest that both Jahn–Teller distortion and charge disproportionation are possible in samples of $LiNiO_2$ at the temperatures at which all the experiments to determine the structure were performed. The Extended X-Ray Absorption Fine Structure (EXAFS) experiments[8] were performed at room temperature; no temperature is reported for the electron diffraction work,[12] but it is reasonable to infer that it was performed at room temperature; the neutron diffraction was performed at a range of temperatures between 10 and 585 K. This may explain the differences in reported experimental structures. Slight changes in the growth conditions, stoichiometry, and other variables could favor the formation of one cell rather than another. It is also possible that both relaxations can occur within the same sample within different grains, for example, or at the surface versus the bulk, or there exists a more stable phase with a complicated charge-orbital ordering pattern, in which Ni^{2+}, Ni^{3+}, and Ni^{4+} coexist.

The $P2/c$ cell matches the majority of the reported experimental findings, two different Ni-O bond lengths, the small monoclinic distortion, the band gap, and the lack of Jahn–Teller-related magnetic properties. Its most important failure is that such a cell should give an approximately 1:1 ratio of the Ni-O short-to-long bonds rather than the approximate ratio of 2:1 observed in Ref. 5 (assuming that we group the Ni-O bond lengths as suggested there). However, if the PDF in Ref. 5 is sampling a mixture of the cells involving charge disproportionation and Jahn–Teller distortion, then our results are consistent with this work since it is clear from the PDF that there is a range of Ni-O distances which contribute to the approximate 2:1 ratio depending on how they are grouped together. We would also have a natural explanation for the domain structure claimed by Ref. 5 at low temperatures.

We turn finally to the magnetic data. Both the data of Ref. 11 and the more recent muon-spin relaxation (μSR) data[42] suggest that the ferromagnetic and antiferromagnetic states are close in energy. The electron spin resonance (ESR) data suggests that the dominant interactions are ferromagnetic, but that strong antiferromagnetic fluctuations exist between 13 and 50 K. However, the saturation of the linewidth suggests that the antiferromagnetic correlations do not propagate below 10 K. The detailed interpretation of the behavior in terms of orbital

TABLE III. Mulliken and Bader charges of nickel and oxide ions in the cells calculated cells. The values in brackets are the volumes (A^3) within which the charge is calculated.

Space group	Mulliken charge (Ni)	Bader charge (Ni)	Bader charge (O)
$R\bar{3}m$	9.229	8.6329 (7.5376)	7.183
$C2/m$	9.335	8.5541 (7.1567)	7.223
$P2_1/c$	9.322	8.5741 (7.182)	7.213
$P2/c$	Ni (a) 9.098	Ni(a) 8.721 (8.279)	O(a) 7.123
	Ni (b) 9.568	Ni(b) 8.515 (6.425)	O(b) 7.259

TABLE IV. Calculated lattice energies per formula unit (meV) relative to the $R\bar{3}m$ cell using a U_{eff} parameter of 6.5 eV. The lowest energy cells are shown in bold. The *Pm* cell is shown in italics since it is unrelaxed.

	$LiNiO_2$	$NaNiO_2$
Pm (experimental coordinates from Ref. 12)	*+61.80*	
$R\bar{3}m$	0	0
$C2/m$	−48.05	**−78.65**
$P2_1/c$	−60.37	−46.28
$P2/c$	**−62.56**	−20.53

frustration is not consistent with later neutron[5] and electron diffraction[12] work. The μSR data predicts different magnetic ground states for different compositions of $Li_{1-x}Ni_xO_2$; ferromagnetic for $x = 0.03$ and 0.15; antiferromagnetic for $x = 0.02$. The authors state that this supports the idea that the change in magnetic state is a bulk effect rather than demonstrating the formation of ferromagnetic or antiferromagnetic domains.

Our calculations cannot fully resolve this issue because of the limited accuracy of density functional theory calculations, but they can illustrate why the complexity exists. We have performed spin-polarized calculations on all the unit cells considered above. The $C2/m$ cell has a ferromagnetic ground state with ferromagnetic coupling, both within the layers and between the layers, but a mixed state with ferromagnetic coupling within the layers, but antiferromagnetic coupling between the layers is only 3 meV above it in energy. For the $P2_1/c$ cell, the ferromagnetic ground state is again lowest, but an antiferromagnetic state is only 5 meV above it. A similar result is obtained for the $P2/c$ cell (which is the one that shows disproportionation of Ni^{3+}) but here, the antiferromagnetic state is only 3 meV above the ferromagnetic ground state. Although the figures apparently predict a ferromagnetic ground state, two points should be noted. First, the density functional calculations are not accurate to a few meV. Second, 1 meV (in terms of kT) corresponds to about 11 K. The calculations are entirely consistent with the great magnetic complexity observed.

IV. CONCLUSIONS

We have calculated three different cells of $LiNiO_2$ and predict a new ground-state crystal structure with $P2/c$ space group symmetry. In this cell, the charge disproportionation reaction $2Ni^{3+} \rightarrow Ni^{2+} + Ni^{4+}$ occurs, which gives two groups of Ni-O bond lengths and the experimentally observed semiconducting behavior. As a result, the ground-state valency of Ni ions should be half $2+$ and half $4+$ charge state. Also the $P2/c$ cell is consistent with the slight monoclinic distortion found at low temperature (10 K). Therefore the absence of cooperative Jahn–Teller distortion is well justified by this cell. Nonetheless, since the energy difference between two mechanisms is extremely small, we cannot exclude the possibility of a trimer ordered system stabilized by local (but still mesoscale) curvature is important. Our results do exclude the possibility that a space group incorporating the trimer ordering (the *Pm* space group suggested by Ref. 12) can be the ground-state configuration. This supports the hypothesis that the mechanism by which individual nickel ions remove orbital degeneracy could easily be influenced by its local environment. This is probable since the various ways of ordering the Jahn–Teller distorted Ni^{3+} ions are all likely to involve significant strain effects caused by local distortion.

In real samples, due to thermal effect and impurities, both Jahn–Teller distortion and charge disproportionation may occur, and the nickel valency could be a mixture of $2+$, $3+$, and $4+$. Ni^{4+} would be expected to show an unusually short Ni-O bond length. This is seen in some of the charge-ordered nickelates (see Table I) and occasionally elsewhere.[43]

Since Ni^{4+} has a very low magnetic moment, this provides an alternative method for relieving the magnetic frustration expected in this compound, but our calculations are not accurate enough to predict the ground magnetic state of the system unambiguously.

Finally, we have illustrated the difference between $LiNiO_2$ and $NaNiO_2$. In $NaNiO_2$, there is only one dominant mechanism which is Jahn–Teller distortion. Here, it is comparably easy to determine its ground-state crystal and electronic structure without any dispute. The different case of $LiNiO_2$, where a number of different possible ground states are very close in energy, illustrates how two systems which are apparently so similar chemically, can nevertheless have very different behavior.

ACKNOWLEDGMENTS

We thank Engineering and Physical Sciences Research Council (EPSRC) for funding under Grant No. EP/G005001/1. Via our membership of the UK's HPC Materials Chemistry Consortium, which is funded by EPSRC (EP/F067496), this work made use of the facilities of HECToR, the UK's national high-performance computing service, which is provided by UoE HPCx Ltd. at the University of Edinburgh, Cray Inc. and NAG Ltd., and funded by the Office of Science and Technology through EPSRC's High End Computing Programme. We thank Keith Refson (STFC, Rutherford-Appleton Laboratory) for useful discussions on the calculations.

*mtp09hc@sheffield.ac.uk

[1] D. Mertz, Y. Ksari, F. Celestini, J. M. Debierre, A. Stepanov, and C. Delmas, Phys. Rev. B **61**, 1240 (2000).

[2] L. A. Montoro, M. Abbate, E. C. Almeida, and J. M. Rosolen, Chem. Phys. Lett. **309**, 14 (1999).

[3] J. S. Kang, S. S. Lee, G. Kim, H. J. Lee, H. K. Song, Y. J. Shin, S. W. Han, C. Hwang, M. C. Jung, H. J. Shin, B. H. Kim, S. K. Kwon, and B. I. Min, Phys. Rev. B **76**, 195122 (2007).

[4] H. Ikeno, I. Tanaka, Y. Koyama, T. Mizoguchi, and K. Ogasawara, Phys. Rev. B **72**, 075123 (2005).

[5]J. H. Chung, Th. Proffen, S. Shamoto, A. M. Ghorayeb, L. Croguennec, W. Tian, B. C. Sales, R. Jin, D. Mandrus, and T. Egami, Phys. Rev. B **71**, 064410 (2005).
[6]M. K. Aydinol, A. F. Kohan, G. Ceder, K. Cho, and J. Joannopoulos, Phys. Rev. B **56**, 1354 (1997).
[7]L. Petit, G. M. Stocks, T. Egami, Z. Szotek, and W. M. Temmerman, Phys. Rev. Lett. **97**, 146405 (2006).
[8]A. Rougier, C. Delmas, and A. V. Chadwick, Solid State Commun. **94**, 123 (1995).
[9]I. Nakai, K. Takahashi, Y. Shiraishi, T. Nakagome, and F. Nishikawa, J. Solid State Chem. **140**, 145 (1998).
[10]J. B. Goodenough, D. G. Wickham, and W. J. Croft, J. Phys. Chem. Solids **5**, 107 (1958).
[11]F. Reynaud, D. Mertz, F. Celestini, J. M. Debierre, A. M. Ghorayeb, P. Simon, A. Stepanov, J. Voiron, and C. Delmas, Phys. Rev. Lett. **86**, 3638 (2001).
[12]J. Cao, H. Zou, C. Guo, Z. Chen, and S. Pu, Solid State Ionics **180**, 1209 (2009).
[13]Z. Chen, H. Zou, X. Zhu, J. Zou, and J. Cao, J. Solid State Chem., doi:10.1016/j.jssc.2011.05.024 (2011).
[14]J. L. Garcia-Munoz, J. Rodriguez-Carvajal, P. Lacorre, and J. B. Torrance, Phys. Rev. B **46**, 4414 (1992).
[15]J. L. Garcia-Munoz, M. A. G. Aranda, J. A. Alonso, and M. J. Martinez-Lope, Phys. Rev. B **79**, 134432 (2009).
[16]J. A. Alonso, M. J. Martinez-Lope, M. T. Casais, J. L. Garcia-Munoz, and M. T. Fernandez-Diaz, Phys. Rev. B **61**, 1756 (2000).
[17]J. A. Alonso, J. L. Garcia-Munoz, M. T. Fernandez-Diaz, M. A. G. Aranda, M. J. Martinez-Lope, and M. T. Casais, Phys. Rev. Lett. **82**, 3871 (1999).
[18]E. Wawrzynska, R. Coldea, E. M. Wheeler, T. Sorgel, M. Jansen, R. M. Ibberson, P. G. Radaelli, and M. Koza, Phys. Rev. B **77**, 094439 (2008).
[19]X. Yang, K. Takada, M. Itose, Y. Ebina, R. Ma, K. Fukuda, and T. Sasaki, Chem. Mater. **20**, 479 (2007).
[20]I. I. Mazin, D. I. Khomskii, R. Lengsdorf, J. A. Alonso, W. G. Marshall, R. M. Ibberson, A. Podlesnyak, M. J. Martınez-Lope, and M. M. Abd-Elmeguid, Phys. Rev. Lett. **98**, 176406 (2007).
[21]W. C. Mackrodt, N. M. Harrison, V. R. Saunders, N. L. Allan, and M. D. Towler, Chem. Phys. Lett. **250**, 66 (1996).
[22]W. C. Mackrodt and D. S. Middlemiss, J. Phys. Cond. Mat. **16**, S2811 (2004).
[23]P. Kuiper, G. Kruizinga, J. Ghijsen, G. A. Sawatzky, and H. Verweij, Phys. Rev. Lett. **62**, 221 (1989).
[24]M. K. Aydinol, A. F. Kohan, G. Ceder, K. Cho, and J. Joannopoulos, Phys. Rev. B **56**, 1354 (1997).
[25]C. A. Marianetti, D. Morgan, and G. Ceder, Phys. Rev. B **63**, 224304 (2001).
[26]K. Mukai, J. Sugiyama, and Y. Aoki, J. Solid State Chem. **183**, 1726 (2010).
[27]V. I. Anisimov, J. Zaanen, and O. K. Andersen, Phys. Rev. B **44**, 943 (1991).
[28]J. P. Perdew, K. Burke, and M. Ernzerhof, Phys. Rev. Lett. **77**, 3865 (1996).
[29]P. E. Blochl, Phys. Rev. B **50**, 17953 (1994).
[30]S. K. Mishra and G. Ceder, Phys. Rev. B **59**, 6120 (1999).
[31]S. L. Dudarev, G. A. Botton, S. Y. Savrasov, C. J. Humphreys, and A. P. Sutton, Phys. Rev. B **57**, 1505 (1998).
[32]F. Zhou, M. Cococcioni, C. A. Marianetti, D. Morgan, and G. Ceder, Phys. Rev. B **70**, 235121 (2004). The reader should note that the values for U_{eff} given there (Table III) are 6.7 eV for Ni^{3+} and 6.04 eV for Ni^{4+}. Our results show that there is no significant difference observed in changing the U_{eff} by a few tenths of an electron volt, and we have chosen 6.5 eV for convenience.
[33]C. Y. Ouyang, S. Q. Shi, and M. S. Lei, J. Alloys Compd. **474**, 370 (2009).
[34]S. Yamamoto and T. Fujiwara, J. Phys. Soc. Jpn. **71**, 1226 (2002).
[35]H.-T. Jeng, G. Y. Guo, and D. J. Huang, Phys. Rev. Lett. **93**, 156403 (2004).
[36]F. Zhou and G. Ceder, Phys. Rev. B **81**, 205113 (2010).
[37]G. Kresse and J. Furthmuller, Phys. Rev. B **54**, 11169 (1996).
[38]W. Li, J. N. Reimers, and J. R. Dann, Solid State Ionics **67**, 123 (1993).
[39]J. Molenda, P. Wilk, and J. Marzec, Solid State Ionics **146**, 73 (2002).
[40]A. V. Krukau, O. A. Vydrov, A. F. Izmaylov, and G. E. Scuseria, J. Chem. Phys. **125**, 224106 (2006).
[41]H. Meskine and S. Satpathy, J Appl. Phys. **97**, 10A314 (2005).
[42]J. Sugiyama, Y. Ikedo, K. Mukai, H. Nozaki, M. Mansson, O. Ofer, M. Harada, K. Kamazawa, Y. Miyake, J. H. Brewer, E. J. Ansaldo, K. H. Chow, I. Watanabe, and T. Ohzuku, Phys. Rev. B **82**, 224412 (2010).
[43]A. N. Mansour, L. Croguennec, and C. Delmas, Electrochem. Solid State Lett. **8**, A544 (2005).